DALTON
FULL PAPER

Synthesis, molecular structure and emission properties of benzoato-bridged lanthanide complexes with hydrotris(pyrazolyl)borate

Udai P. Singh,*[a] **Shalu Tyagi,**[a] **Chokhe Lal Sharma,**[a] **Helmut Görner**[b]
and Thomas Weyhermüller*[b]

[a] *Department of Chemistry, Indian Institute of Technology Roorkee, Roorkee, 247 667, India.*
E-mail: udaipfcy@iitr.ernet.in
[b] *Max-Planck-Institut für Strahlenchemie, D-45413 Mülheim an der Ruhr, Germany*

Received 24th May 2002, Accepted 20th September 2002
First published as an Advance Article on the web 25th October 2002

Reaction of $GdCl_3$ and $TbCl_3$ with one equivalent of the potassium salt of the tridentate ligand hydrotris(pyrazol-1-yl)borate [K(tp)] and two equivalents of sodium *p*-X-benzoate (X = H, Cl, Br and NO_2) yielded the complexes **1**–**6** of composition $[\{(tp)Ln(\mu\text{-}p\text{-X-OBz})_2\}_2]$ (Ln = Gd, Tb) whereas the reaction of $TbCl_3$ with 2 equivalents of [K(tp)] and one equivalent of sodium azide, gave the tetranuclear complex $[\{(tp)_2Tb(\mu\text{-}N_3)\}_4]$ (**7**). The crystal structures of the benzoate complexes (X = H) of Gd (**1**) and Tb (**2**) and their analogous *p*-Cl-benzoate derivatives with Gd (**3**) and Tb (**4**) have been determined. The compounds consist of a seven-coordinate tetrakis carboxylato bridged dimetal unit with two capping hydrotris(pyrazolyl)borate ligands. Unit cell determinations suggested that $[\{(tp)Tb(\mu\text{-}p\text{-Cl-OBz})_2\}_2]$ (**5**), and $[\{(tp)Tb(\mu\text{-}p\text{-}NO_2\text{-OBz})_2\}_2]$ (**6**), are isostructural with (**3**) and (**4**). Single crystal X-Ray analysis of (**7**) revealed its tetranuclear structure comprising a cyclic 16-membered $Tb_4(\mu\text{-}N_3)_4$-unit with two hydrotris(pyrazol-1-yl)borate ligands bound to each of the terbium ions resulting in a tetragonal antiprismatic N_8-coordination sphere. The luminescence properties of the unsubstituted and *para*-substituted Gd and Tb benzoate complexes have been studied in solution at room temperature.

Introduction

The coordination chemistry of lanthanides has become a more attractive subject in the last several years due to their wide variety of potential applications. In particular Eu(III) and Tb(III) are characterized by their long-lived (millisecond time-scale) strongly luminescent electronically excited states, which makes them appealing for analytical purposes. Luminescent complexes of Eu(III) and Tb(III) may be useful in medicine as luminescent probes[1] and highly paramagnetic complexes, generally of Gd(III), are used as contrast agents to enhance the output from magnetic resonance imaging (MRI) scanners.[2] Eu(III) and Tb(III) complexes are able to transfer the energy absorbed by the organic ligand to the lanthanide cation which shows a characteristic luminescence with narrow bands in the green and red spectral range.[3–12] The luminescence lifetime (τ_{em}) of several Eu and Tb complexes, *e.g.* with tris(pyrazolyl)borate ligands[10–12] is in the ms time range and sensitive to the medium. The occurrence of an antenna effect, which allows sensitization of the metal centered luminescence *via* energy transfer from an aromatic ligand which acts as light harvester, means that lanthanide complexes with aromatic ligands are of interest for supramolecular light-conversion devices.[13] In order to exploit this luminescence, the lanthanide ions must be coordinated to a suitable multidentate ligand in order to:

(i) populate the lanthanide emitting level taking advantage of a large ligand absorption cross section, followed by ligand-to-metal energy transfer, because the lanthanide f–f excited states are not readily accessible by direct excitation; and

(ii) protect the ion coordination sphere from solvent interactions, which can deactivate its excited state *via* non-radiative processes.[1]

Several research groups have put much effort into designing well tailored ligands, and a great variety of them are now available in the literature. In general, one can say that small variations in a ligand structure can lead to remarkable changes in the photophysical properties.

Many types of lanthanide carboxylates have been reported.[14] The carboxylates show interesting polymeric network and chain structures, few of them fluoresce and only one example of hydrotris(pyrazolyl)borate with yttrium and acetate is available in the literature[14a] prior to this work where four benzoate groups are acting as bridging ligands. Also the azido anion serves as a versatile bridging ligand which can coordinate to metal ions giving several kinds of complexes in either end-to-end (EE) or end-on (EO) fashion.[15] To the best of our knowledge, no such kind of azido bridged complex with rare earth metal centers as tetramers has been synthesized and characterized crystallographically except for one recently reported complex which has not been properly characterized.[16]

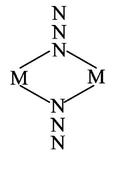

end-on

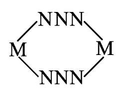

end-to-end

It is clearly demonstrated in the literature that a relatively modest change in the ligand structure can give dramatic variations in the luminescence properties of the corresponding lanthanide complexes, which in turn suggests that the search for ligands which exactly optimize the useful properties of lanthanide complexes is still a challenging task. There is therefore considerable interest in the development of new lanthanide complexes with suitable photophysical properties for their application. We have prepared lanthanide complexes with hydrotris(pyrazolyl)borate by using different bridging ligands.

DOI: 10.1039/b205053f

The present paper reports the synthesis, molecular structure, and luminescence studies of the complexes [(tp)Gd(μ-OBz)$_4$Gd(tp)]·CH_2Cl_2 (**1**), [(tp)Tb(μ-OBz)$_4$Tb(tp)]·CH_2Cl_2 (**2**), [(tp)Gd(μ-*p*-Cl-OBz)$_4$Gd(tp)]·4CH_2Cl_2 (**3**), [(tp)Tb(μ-*p*-X-OBz)$_4$Tb(tp)], where X = Cl (**4**), Br (**5**) and NO_2 (**6**) and [{$(tp)_2$Tb(μ-N_3)}$_4$]·6CH_2Cl_2 (**7**).

Experimental

All solvents were predried from appropriate drying agents by the literature methods.[17] The benzoic acid and *p*-X-benzoic acid (X = Cl, Br or NO_2) were commercially available and their sodium salts were prepared by reacting with the appropriate amount of sodium hydroxide in water. All the lanthanide chlorides of the highest grade were purchased from Indian Rare Earths Ltd., India. The potassium salt of the ligand hydrotris(pyrazol-1-yl)borate (tp) was prepared by published procedures.[18]

Physical measurements

Infrared spectra (400–4000 cm^{-1}) of solid samples were recorded on a Perkin-Elmer model 1600 FT-IR spectrometer as KBr disks. Electro Spray Ionization mass spectra (ESI-MS) in the positive ion mode were recorded on a Hewlett-Packard HP 5989 mass spectrometer. The used solvent is given in parentheses. The intensity and possible composition of the peaks is between parentheses. Temperature dependent magnetic susceptibilities of powdered samples were measured by using a SQUID magnetometer (Quantum Design) at 1.0 T (2–290 K). Corrections for underlying diamagnetism were made by using tabulated Pascal constants.

Steady-state measurements were performed using an absorption spectrophotometer (HP 8453 diode array) and spectrofluorimeters (Varian Cary Eclipse, Spex-Fluorolog and Perkin Elmer, LS-5).[19] Absorbances of 0.5–1.0 at λ_{exc} = 230–310 nm) were used throughout. The quantum yield of emission was measured using optically matched solutions and the fluorescence of 9,10-diphenylanthracene in EtOH ($\Phi_f = 0.6$) as reference. The same emission lifetime was obtained with either the Perkin Elmer spectrofluorimeter or the laser flash photolysis set-up (λ_{exc} = 248 or 308 nm),[19] when the laser intensity was low enough. In several cases, *e.g.* **2** in dichloromethane, no effect of the absence or presence of oxygen on the lifetime was found.

X-Ray crystallographic data collection and refinement of the structures

Colorless single crystals of **1**, **2** and **4** were coated with perfluoropolyether, picked up with glass fibers, and mounted on a Siemens Smart-CCD diffractometer. Crystals of **3** and **7** were treated the same way but mounted on a Nonius Kappa-CCD diffractometer with a rotating Mo-anode setup. Both systems were equipped with a nitrogen cold stream operating at 100(2) K. Graphite monochromated Mo Kα radiation (λ = 0.71073) was used throughout. Crystallographic data are listed in Table 1. Cell constants were obtained from a least square fit of diffraction angles of several thousand strong reflections. Intensity data were corrected for Lorentz and polarization effects. Crystal faces were determined and the face-indexed correction routine embedded in ShelXTL[20] was used to account for absorption. The Siemens ShelXTL[20] software package was used for solution, refinement and artwork of the structures and neutral atom scattering factors of the program were used. Non-hydrogen atoms were refined anisotropically and hydrogen atoms were placed at calculated positions and refined as riding atoms with isotropic displacement parameters.

All structures appeared to be well ordered except a CH_2Cl_2 solvent molecule in crystals of **7** which was found to be disordered over two sites. A split atom model with restrained C–Cl bond distances and occupation factors of 0.58 and 0.42 gave satisfactorily results.

CCDC reference numbers 186521–186525.

See http://www.rsc.org/suppdata/dt/b2/b205053f/ for crystallographic data in CIF or other electronic format.

Preparation of complexes

[(tp)Gd(μ-OBz)$_4$Gd(tp)]·CH_2Cl_2 (1). A mixture of sodium benzoate (0.288 g, 2.00 mmol) and [K(tp)] (0.252 g, 1.00 mmol) in 20.0 ml of methanol was added to the methanolic solution of $GdCl_3·6H_2O$ (0.371 g, 1.00 mmol). The suspension was stirred at room temperature for 3–4 h. After removal of the solvent under vacuum, the residue was extracted with CH_2Cl_2 (50.0 ml) and the solution was filtered to eliminate the salt. The filtrate was dried under vacuum to afford a colorless powder solid (83.0%, 0.508 g, 0.41 mmol). Recrystallization of the resulting solid from CH_2Cl_2–hexane at 4 °C gave crystals suitable for X-ray measurements. The elemental analysis was performed on a carefully dried sample under vacuum for several hours. Anal. Calc. for $C_{46}H_{40}N_{12}O_8B_2Gd_2$: C, 45.10; H, 3.29; N 13.72. Found: C, 44.90; H, 3.50; N, 14.10%. IR (KBr, cm^{-1}): 2455 (*ν*BH), 1605 (ν_{as}COO), 1505 (ν_sCOO). MS (ESI+, CH_2Cl_2): *m*/*z* 1104 (35.0%) [$(tp)_2Gd_2(O_2CPh)_3$]$^+$, 704 (0.2%) [$(tp)_2Gd(O_2CPh)$ + H]$^+$, 584 (100.0%) [$(tp)_2$Gd]$^+$. Magnetic moment μ_{eff} (290 K): 10.32 μ_B, μ_{eff} (2 K): 8.53 μ_B.

[(tp)Tb(μ-OBz)$_4$Tb(tp)]·CH_2Cl_2 (2). This complex was prepared in 82.0% (0.502 g, 0.41 mmol) yield as outlined above for (**1**). Anal. Calc. for $C_{46}H_{40}N_{12}O_8B_2Tb_2$: C, 44.98; H, 3.28; N 13.68. Found: C, 44.58; H, 3.20; N, 13.25%. IR (KBr, cm^{-1}): 2455 (*ν*BH), 1611 (ν_{as}COO), 1505 (ν_sCOO). MS(ESI+, CH_2Cl_2): *m*/*z* 1107 (2.0%) [$(tp)_2Tb_2(O_2CPh)_3$]$^+$; 729 (0.4%) [$(tp)_2Tb(O_2CPh)$ + Na]$^+$; 585 (100.0%) [$(tp)_2$Tb]$^+$. Magnetic moment μ_{eff} (290 K): 11.48 μ_B, μ_{eff} (2 K): 6.73 μ_B.

[(tp)Gd(μ-*p*-Cl-OBz)$_4$Gd(tp)]·4CH_2Cl_2 (3). This complex was prepared in 72.8% (0.583 g, 0.43 mmol) yield as outlined above for (**1**). Anal. Calc. for $C_{46}H_{36}N_{12}O_8B_2Cl_4Gd_2$: C, 40.54; H, 2.66; N 12.33. Found: C, 39.21; H, 2.72; N, 12.46%. IR (KBr, cm^{-1}): 2455 (*ν*BH), 1600 (ν_{as}COO), 1500 (ν_sCOO). MS(ESI+, CH_2Cl_2): *m*/*z* 1208 (0.4%) [$(tp)_2Gd_2$(*p*-Cl-$O_2CPh)_3$]$^+$; 762 (3.0%) [$(tp)_2$Gd(*p*-Cl-O_2CPh) + Na]$^+$; 584 (100.0%) [$(tp)_2$Gd]$^+$. Magnetic moment μ_{eff} (290 K): 10.19 μ_B, μ_{eff} (2 K): 8.36 μ_B

[(tp)Tb(μ-*p*-Cl-OBz)$_4$Tb(tp)]·4CH_2Cl_2 (4). This complex was prepared in 81.7% (0.605 g, 0.44 mmol) yield as outlined above for (**1**). Anal. Calc. for $C_{46}H_{36}N_{12}O_8B_2Cl_4Tb_2$: C, 40.44; H, 2.65; N 12.30. Found: C, 39.91; H, 2.54; N, 12.16%. IR (KBr, cm^{-1}): 2455 (*ν*BH), 1611 (ν_{as}COO), 1505 (ν_sCOO). MS(ESI+. CH_2Cl_2): *m*/*z* = 1211 (4.0%) [$(tp)_2Tb_2$(*p*-Cl-$O_2CPh)_3$]$^+$; 763 (52.0%), [$(tp)_2$Tb(*p*-Cl-O_2CPh) + Na]$^+$; 585 (55.0%) [$(tp)_2$Tb]$^+$. Magnetic moment μ_{eff} (290 K): 13.05 μ_B, μ_{eff} (2 K): 7.50 μ_B.

[(tp)Tb(μ-*p*-Br-OBz)$_4$Tb(tp)] (5). This complex was prepared in 82.0% (0.631 g, 0.40 mmol) yield as outlined above for (**1**). Anal. Calc. for $C_{46}H_{36}N_{12}O_8B_2Br_4Tb_2$: C, 35.78; H, 2.35; N 10.88. Found: C, 35.49; H, 2.39; N, 10.57%. IR (KBr, cm^{-1}): 2444 (*ν*BH), 1605 (ν_{as}COO), 1505 (ν_sCOO). MS(ESI+. CH_2Cl_2): *m*/*z* = 1343 (0.2%) [$(tp)_2Tb_2$(*p*-Br-$O_2CPh)_3$]$^+$; 784 (9.0%) [$(tp)_2$Tb(*p*-Br-O_2CPh) + H]$^+$; 585 (100.0%) [$(tp)_2$Tb]$^+$. Magnetic moment μ_{eff}(290 K): 13.62 μ_B, μ_{eff} (2 K): 7.83 μ_B.

[(tp)Tb(μ-*p*-NO_2-OBz)$_4$Tb(tp)] (6). This complex was prepared in 85.0% (0.601 g, 0.43 mmol) yield as outlined above for (**1**). Anal. Calc. for $C_{46}H_{36}N_{16}O_{16}B_2Tb_2$: C, 39.23; H, 2.57; N 15.91. Found: C, 39.04; H, 2.48; N, 16.03%. IR (KBr, cm^{-1}): 2444 (*ν*BH), 1605 (ν_{as}COO), 1505 (ν_sCOO). MS(ESI+, CH_2Cl_2): *m*/*z* 1336 (10.0%) [$(tp)_4Tb_2$(*p*-NO_2-O_2CPh)]$^+$; 1242

Table 1 Crystallographic data for **1**·CH_2Cl_2, **2**·CH_2Cl_2, **3**·4CH_2Cl_2, **4**·4CH_2Cl_2 and **7**·6CH_2Cl_2,

	1·CH_2Cl_2	**2**·CH_2Cl_2	**3**·4CH_2Cl_2	**4**·4CH_2Cl_2	**7**·6CH_2Cl_2
Chem, formula	$C_{47}H_{42}B_2Cl_2Gd_2N_{12}O_8$	$C_{47}H_{42}B_2Cl_2Tb_2N_{12}O_8$	$C_{50}H_{44}B_2Cl_{12}Gd_2N_{12}O_8$	$C_{50}H_{44}B_2Cl_{12}N_{12}O_8Tb_2$	$C_{78}H_{92}B_8Cl_{12}N_{60}Tb_4$
M_w	1309.94	1313.29	1702.49	1705.83	3017.68
Space group	$P\bar{1}$, no. 2	$P\bar{1}$, no. 2	$P\bar{1}$, no. 2	$P\bar{1}$, no. 2	$P2_1/c$, no. 14
a/Å	12.5351(8)	12.5382(9)	9.3945(5)	9.4247(7)	15.8429(4)
b/Å	13.0435(8)	13.0146(9)	12.6965(8)	12.7294(8)	25.3237(8)
c/Å	16.3461(12)	16.3211(12)	14.2564(9)	14.274(2)	15.9930(8)
α/°	72.56(1)	72.71(1)	74.75(1)	74.74(1)	90
β/°	83.37(1)	83.64(1)	76.04(1)	76.25(1)	115.06(1)
γ/°	89.58(1)	89.57(1)	83.29(1)	83.30(1)	90
V/Å^3	2531.7(3)	2526.4(3)	1589.5(2)	1602.1(3)	5812.4(4)
Z	2	2	1	1	2
T/K	100(2)	100(2)	100(2)	100(2)	100(2)
D_c/g cm^{-3}	1.718	1.726	1.779	1.768	1.724
μ(Mo-Kα)/cm^{-1}	27.67	29.47	26.33	27.49	27.50
Diffractometer used	Siemens SMART	Siemens SMART	Nonius Kappa-CCD	Siemens SMART	Nonius Kappa-CCD
Refl. collected	28063	27882	17689	17660	66553
Unique refl./[$I > 2\sigma(I)$]	16662/12664	16579/13087	12046/11339	10605/7675	22022/17192
No. parameters/restraints	658	658	388	388	747/6
θ range/°	1.64–33.18	1.63–33.16	2.63–33.18	1.66–33.81	2.56–33.13
$R1^a/wR2^b$ [$I > 2\sigma(I)$]	0.0292/0.0553	0.0273/0.0584	0.0404/0.1067	0.0564/0.1150	0.0343/0.0664
GooF^c	0.917	0.927	1.064	0.992	1.022
Residual density/e Å^{-3}	+1.298/−1.137	+1.547/−1.586	+2.928/−2.239	+1.510/−1.834	+1.004/−1.215

[a] $R1 = \Sigma||F_o| - |F_c||/\Sigma|F_o|$. [b] $wR2 = [\Sigma[w(F_o^2 - F_c^2)^2]/\Sigma[w(F_o^2)^2]]^{1/2}$ where $w = 1/\sigma^2(F_o^2) + (aP)^2 + bP$, $P = (F_o^2 + 2F_c^2)/3$ [c] GooF = $[\Sigma[w(F_o^2 - F_c^2)^2]/(n - p)]^{1/2}$ where n = no. of Refl. and p = no. of refined param.

(0.4%), $[(tp)_2Tb_2(p\text{-}NO_2\text{-}O_2CPh)_3]^+$; 774 (3.0%) $[(tp)_2Tb(p\text{-}NO_2\text{-}O_2CPh) + Na]^+$; 585 (100.0%) $[(tp)_2Tb]^+$. Magnetic moment μ_{eff} (290 K): 12.32 μ_B, μ_{eff} (2 K): 7.06 μ_B.

[{(tp)$_2$Tb(μ-N$_3$)}$_4$]·6CH$_2$Cl$_2$ (7). A methanolic solution (10 ml) of sodium azide (0.065 g, 1.00 mmol) was added to a stirred methanolic solution (15 ml) of [K(tp)] (0.504 g, 2.00 mmol) and $TbCl_3 \cdot 6H_2O$ (0.373 g, 1.00 mmol). The resulting mixture was stirred for 4 h and methanol was evaporated to dryness under vacuum. The solid product was extracted with CH_2Cl_2 (3 × 10 ml) and the extracted dichloromethane solution was filtered on Celite. The solvent was evacuated under vacuum and colourless powdered solid in 89.0% (0.558 g, 0.22 mmol) yield was recrystallized from CH_2Cl_2–hexane at 4 °C. The elemental analysis was performed after complete drying the sample under vacuum for several hours. Anal. Calc. for $C_{72}H_{80}N_{60}B_8Tb_4$: C, 34.48; H, 3.21; N, 33.51. Found: C, 34.16; H, 3.17; N, 33.27%. IR (KBr, cm^{-1}): 2455 (νBH), 2122 (νN_3). MS(ESI+, DMF): *m/z* 2296 (very weak) $[(tp)_7Tb_4(N_3)_4]^+$; 1840 (0.5%) $[(tp)_6Tb_3(N_3)_2]^+$; 1212 (0.6%) $[(tp)_4Tb_2N_3]^+$; 585 (100.0%) $[(tp)_2Tb]^+$. Magnetic moment μ_{eff} (290 K): 17.98 μ_B, μ_{eff} (2 K): 10.17 μ_B.

Results and discussion

The syntheses of the complexes **1**–**7**, were carried out by the stoichiometric combination of Gd/$TbCl_3$ and the appropriate ligand salts in methanol, *i.e.* MCl_3 (1.0 mmol), [K(tp)] (2.0 mmol) and sodium benzoate/sodium-*p*-X-benzoate (2.0 mmol) or sodium azide (1.0 mmol). Reaction of tp as its potassium salt with lanthanide(III) chloride in presence of sodium *p*-X-benzoate resulted in complexes of the form $[\{(tp)Ln(\mu\text{-}p\text{-}X\text{-}OBz)_2\}_2]$ whereas in the presence of sodium azide, the reaction of tp with terbium chloride resulted the formation of a tetramer $[\{(tp)_2Tb(\mu\text{-}N_3)\}_4]$. In case of $[\{(tp)Ln(\mu\text{-}p\text{-}X\text{-}OBz)_2\}_2]$ (Ln = Gd or Tb, X = H, Cl, Br or NO_2), one ligand is coordinated to a single metal center, which accounts for seven coordination sites whereas in complex **7** two tp ligands are coordinated to a single metal center, providing a tetragonal antiprismatic N8-coordination sphere. The remaining sites in complexes **1**–**6** are occupied by four carboxylate groups and in **7** by two azido groups. All complexes were characterized by ESI mass spectroscopy, elemental analysis, infrared, and in the cases of **1**–**4** and **7**, X-ray crystallography.

Infrared spectra

IR studies indicate that bands present in the complexes, but not in the free ligand, in the range of 1611–1600 and 1505–1500 cm^{-1} assigned to asymmetric (ν_{as}) and symmetric (ν_s) stretching vibrations of the carboxyl group, respectively. The IR spectra are very similar across the series and show only one B–H stretching vibration. Comparison of the IR spectra for benzoate or *p*-X-benzoate with each other revealed that in all these complexes, **1**–**6**, the carboxylate groups are coordinated in the same fashion, *i.e.* in bidentate fashion. The confirmation of the coordination mode of the carboxylate groups were again provided crystallographically. In complex **7**, the presence of νN=N band at 2122 cm^{-1} suggests the coordination of azide in 1,3-bridging mode[21] and is in the usual range for end-to-end bridging N-bonded azide anions.[15,16]

Crystallographic studies

Molecular structure of [(tp)Gd(μ-OBz)$_4$Gd(tp)]·CH$_2$Cl$_2$ (1). The solid structure of **1** has been determined by X-ray crystallography. Fig. 1 shows an ORTEP diagram of **1** on a 50% probability level. Table 2 lists selected bond lengths and bond angles for it. The complex crystallizes in the triclinic space group $P\bar{1}$ (Z = 2). The unit cell consists of two crystallographically independent complex molecules each lying on a center of inversion and two dichloromethane solvate molecules. The gadolinium atoms are in an unusual seven-coordinate environment, each gadolinium atom is coordinated by four oxygen atoms from the benzoate ligands and three nitrogen atoms from a tris(pyrazolyl)borate ligand as shown in Fig. 1. The gadolinium atoms are separated by 3.9430(4) Å, and the gadolinium–oxygen bond distances are found between 2.288(2) and 2.382(2) Å which are well within the range as reported in the literature for tetra-carboxylato bridged complex but slightly smaller than found for complexes where three or two carboxylates are present as bridging ligands.[14] Structural studies of rare earth carboxylates[14] have shown that the carboxylate groups may be coordinated simultaneously in three modes, namely, chelating, bridging and chelating–bridging. In the present structure, the X-ray study shows that two carboxylates form a normal μ_2-mode and two carboxylates coordinate in a more chelating–bridging mode within the dimeric unit as can be seen

Table 2 Selected bond lengths (Å) and angles (°)

	Gd (**1**)	Tb (**2**)	Gd (**3**)	Tb (**4**)
M(1)–N(2)	2.507(2)	2.491(2)	2.513(2)	2.505(4)
M(1)–N(7)	2.530(2)	2.517(2)	2.479(2)	2.473(4)
M(1)–N(12)	2.498(2)	2.483(2)	2.528(2)	2.527(4)
M(1)–O(16)	2.382(2)	2.362(2)	2.353(2)	2.344(3)
M(1)–O(17)#1	2.288(2)	2.264(2)	2.303(2)	2.291(3)
M(1)–O(17)	2.872(2)	—	2.808(2)	2.850(3)
M(1)–O(23)	2.321(2)	2.305(2)	2.317(2)	2.311(3)
M(1)–O(24)#1	2.331(2)	2.318(2)	2.311(2)	2.303(3)
M(1)–M(1)#1	3.9430(4)	3.9458(4)	3.9148(4)	3.9242(7)
O(17)#1–M(1)–O(23)	78.77(6)	79.39(6)	78.14(7)	78.45(12)
O(17)#1–M(1)–O(24)#1	78.82(6)	79.20(6)	79.71(7)	80.30(12)
O(23)–M(1)–O(24)#1	134.54(6)	133.91(6)	134.29(7)	133.62(12)
O(17)#1–M(1)–O(16)	129.17(6)	129.33(6)	129.98(7)	129.93(12)
O(23)–M(1)–O(16)	85.65(6)	84.60(6)	82.12(8)	81.34(12)
O(24)#1–M(1)–O(16)	78.77(6)	78.35(6)	82.34(8)	81.59(12)
O(17)#1–M(1)–O(17)	80.96(6)	—	80.50(7)	81.05(11)
O(23)–M(1)–O(17)	68.66(5)	—	68.51(7)	68.19(11)
O(24)#1–M(1)–O(17)	69.09(5)	—	68.72(7)	68.09(10)
O(16)–M(1)–O(17)	48.43(5)	—	49.49(6)	48.89(11)
O(17)#1–M(1)–N(12)	158.58(7)	158.16(6)	89.00(8)	88.56(12)
O(23)–M(1)–N(12)	101.45(6)	100.98(6)	73.29(7)	73.67(12)
O(24)#1–M(1)–N(12)	113.35(6)	113.51(6)	145.39(8)	146.10(12)
O(16)–M(1)–N(12)	71.85(6)	72.06(6)	128.00(8)	128.22(12)
O(17)#1–M(1)–N(2)	92.33(6)	91.86(7)	84.46(8)	83.96(13)
O(23)–M(1)–N(2)	144.92(6)	145.80(6)	142.59(8)	143.20(12)
O(24)#1–M(1)–N(2)	74.81(6)	75.01(6)	72.87(8)	73.23(12)
O(16)–M(1)–N(2)	124.22(6)	124.49(6)	132.97(8)	133.38(13)
N(12)–M(1)–N(2)	75.10(7)	75.49(7)	73.54(8)	73.82(13)
O(17)#1–M(1)–N(7)	84.69(7)	83.90(7)	155.01(8)	154.72(13)
O(23)–M(1)–N(7)	73.35(6)	73.58(6)	113.23(8)	113.41(13)
O(24)#1–M(1)–N(7)	142.15(6)	142.77(6)	103.55(8)	103.18(13)
O(16)–M(1)–N(7)	136.00(6)	136.19(6)	74.76(7)	75.10(12)
N(12)–M(1)–N(7)	75.03(7)	75.42(7)	74.23(8)	74.58(13)
N(2)–M(1)–N(7)	72.07(7)	72.64(7)	73.20(8)	73.43(13)

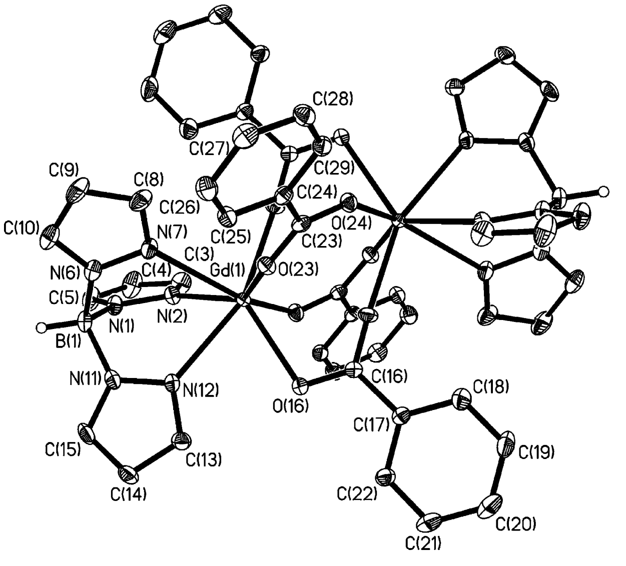

Fig. 1 Molecular structure of [(tp)Gd(μ-OBz)$_4$Gd(tp)] (**1**) drawn at the 50% probability level. All hydrogen atoms and the solvent molecule have been omitted for clarity.

from the differences in bond distances of Gd–O of coordinated benzoate (Table 2). The two Gd–O [Gd(1)–O(16) and Gd(1)–O(24)] bond lengths on one side of Gd(1)–Gd(1′) are slighty longer than two Gd–O [Gd(1)–O(17) and Gd(1)–O(23)] bond distances on the other side. The gadolinium–nitrogen bond distances of the coordinated pyrazolylborate ligand are in the range 2.498(2)–2.530(2) Å. The Gd(1)–N(7) bond distance is slightly longer [2.530(2) Å] than the Gd(1)–N(12) [2.498(2) Å] and Gd(1)–N(2) [2.507(2) Å]. The average C–C bond distance in the aromatic ring of the benzoate ligand is 1.38 Å.

The benzoate complex of terbium (**2**) is isomorphous and isostructural with the gadolinium complex and crystallizes in the triclinic crystal system with the same space group of $P\bar{1}$.

Molecular structure of [{(tp)Tb(μ-p-Cl-OBz)$_2$}$_2$]·4CH$_2$Cl$_2$ (4). The molecular structure and atomic numbering of the complex **4** is shown in Fig. 2. The bond distances and angles are listed in Table 2. The dinuclear entity is centrosymmetric with four bridging carboxylate groups as **1** but this time the unit cell contains one complex molecule lying on a crystallographic inversion center and four dichloromethane solvate molecules. Each terbium ion is linked to seven atoms, four oxygen atoms from bridging carboxylate groups,where the bridging mode is very similar to **1**, and three nitrogen atoms from a pyrazolylborate ligand. The Tb–Tb bond distance in this complex is 3.9242(7) Å, which is slightly shorter than in complex **2**, *i.e.*, 3.9458(4) Å. The average Tb–O [Tb(1)–O(17), Tb(1)–O(24), Tb(1)–O(23) and Tb(1)–O(16)] bond distance formed by the bridging carboxylates in present complex is 2.312 Å whereas the average Ln–O bond distance found with the chelating carboxylate groups in the lanthanide complexes is 2.543 Å. The average Tb–O bond found in complex **4** is the same as in complex **2** *i.e.*, 2.312 Å, but a little smaller than the corresponding average distances, 2.369 Å, found in the Eu–benzoate complex.[14] The average bond length of Tb–N in the present complex is 2.501 Å which is slightly smaller than average Eu–N distance, 2.637 Å in Eu(p-mba)$_3$(bpy) complex, but larger than in complex **2**, *i.e.*, 2.497 Å. These indicate that interaction between the terbium ion and the oxygen atoms in complexes **4** and **2** are of equal strength but weaker than that in [Eu(p-moba)$_3$(bpy)]·

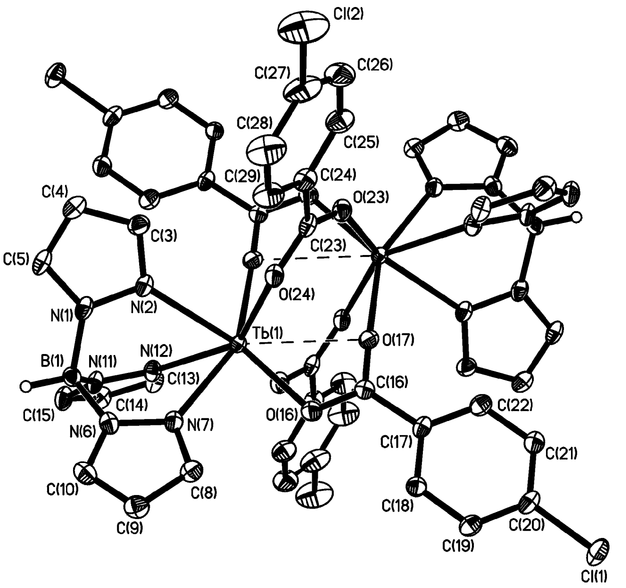

Fig. 2 Molecular structure of [(tp)Tb(μ-*p*-Cl-OBz)$_4$Tb(tp)] (**4**) drawn at the 50% probability level. All hydrogen atoms and the solvent molecule have been omitted for clarity.

$0.5C_2H_5OH$ and in the [Eu(*p*-mba)$_3$(bpy)] complex. The interaction between the terbium ion and nitrogen atom in **4** is stronger than in complex **2** but weaker than in the Eu(*p*-mba)$_3$(bpy) complex.

Like complex **1** and **2**, complex **3** is also isomorphous and isostructural with terbium complex **4**. In complex **3**, the Gd–Gd bond distance is 3.9148(4) Å and both gadolinium ions are seven coordinate, forming a dimeric unit.

Molecular structure of [{(tp)$_2$Tb(μ-N$_3$)}$_4$]·6CH$_2$Cl$_2$ (7). The single-crystal X-ray diffraction studies confirmed the formulation of complex **7** as being [{(tp)$_2$Tb(μ-N$_3$)}$_4$]. The molecular structure of **7** (Fig. 3) consists of a tetrameric cycle of (tp)$_2$TbN$_3$ units owing a crystallographic center of inversion. The terbium ions in the tetramer are linked by one end-to-end bridging azide ion. Each terbium ion is eight-fold coordinated with six nitrogen atoms from two tp ligands and two nitrogen atoms from bridging azide ions, and exhibits a distorted square antiprism, with twist angles of 39.5° at Tb(1) and 37.6° at Tb(2), with the coordination sphere as shown in Fig. 3. There are several examples of lanthanide complexes with tp ligands which are all eight coordinate (two tp ligands plus a bidentate or two unidentate ligands). All the terbium ions in present complex are in similar coordination environments with Tb–Tb distance of 6.531(1) Å. The Tb–N (from bridging azide) bond distances are in the range 2.423(2) [Tb(1)–N(80)] to 2.450(2) [Tb(2)–N(82)] Å (Table 3) which are significantly shorter than generally observed.[22a,22e] Similar bidentate coordination behavior of azide ions to lanthanides has been observed by other workers also but most the of reported lanthanide azide complexes are dimers or polymers.[16,22] The Tb–N bond distances from the coordinated tp ligands of 2.458(2) Å [Tb(1)–N(32)], 2.500(2) Å [Tb(1)–N(12)], 2.507(2) Å [Tb(1)–N(22)], 2.520(2) Å [Tb(1)–N(7)], 2.534(2) Å [Tb(1)–N(27)], 2.545(2) Å [Tb(1)–N(2)] are somewhat shorter than the distances of 2.583(3)–2.664(3) Å, reported for other eight-coordinated lanthanide complexes with tp ligands.[11,12,14a,b]

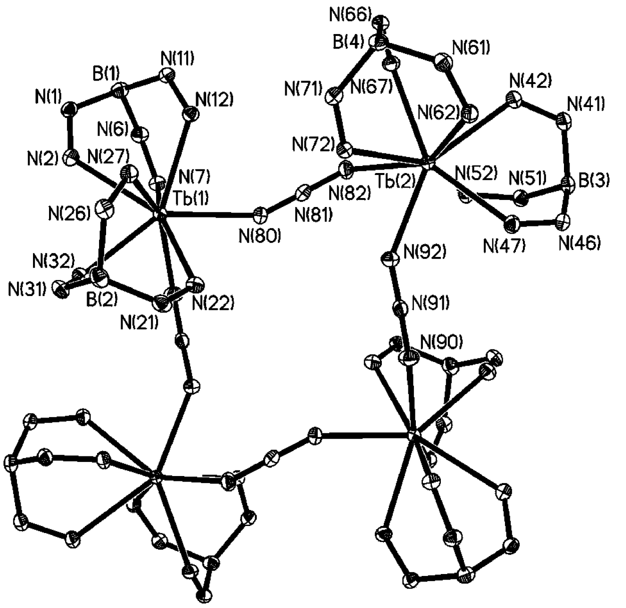

Fig. 3 Molecular structure of [{(tp)$_2$Tb(μ-N$_3$)}$_4$] (**7**) drawn at the 50% probability level. All hydrogen atoms and the solvent molecule have been omitted for clarity.

Emission properties

Emission intensity and lifetime. The emission spectrum of the Tb complex **2** in dichloromethane at room temperature exhibits specific maxima at *ca.* 490, 545, 590 and 620 nm; the peak width at 545 nm is *ca.* 300 cm^{-1} and the intensity ratio is *ca.* 0.5:1:0.1:0.05, respectively. The spectral peaks are due to the $^5D_5 \longrightarrow {}^7F_j$ transitions.[4–6] In cyclohexane (Fig. 4), acetonitrile or ethanol the maxima and intensity ratios are similar. Variation of the bridging ligands of the Tb complexes causes changes of the peak intensity (I_{em}) *e.g.* at 545 nm, but virtually no spectral changes (Table 4). Taking I_{em} as a measure of the relative quantum yield of emission, it follows that population of the emitting state is substantial for **4** and **7**, but rather small for the *p*-nitrobenzoate **6**. The quantum yield of emission was estimated to be $\Phi_{em} = 0.12$ for **2** in dichloromethane.

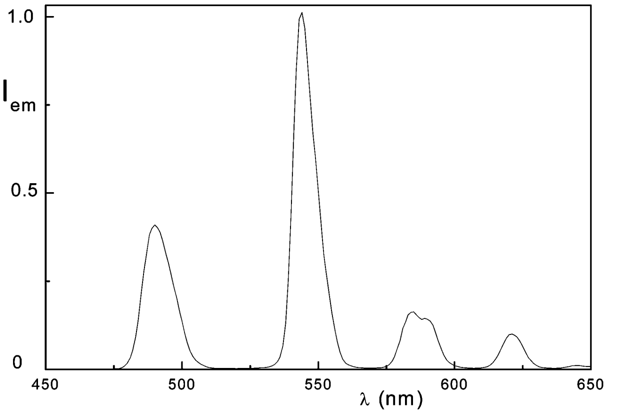

Fig. 4 Emission spectrum of [(tp)Tb(μ-OBz)$_4$Tb(tp)] (**2**) in air-saturated cyclohexane, λ_{exc} = 250 nm.

The luminescence excitation spectra of **2**, **4**, **5** and **7** agree with the absorption spectrum which steadily decreases with λ (at 200–300 nm), exhibiting a shoulder around 240 nm. An exception from this pattern is **6**, having also a weak band in absorption and luminescence excitation around 270 nm. In contrast to the Tb complexes, no emission could be detected for the Gd complexes (**1** and **3**) in dichloromethane, under otherwise the same conditions.

The lifetime of the first-order emission decay of the Tb complexes is typically τ_{em} = 1.6–1.7 ms. Variation of the bridging ligands in dichloromethane or variation of the solvent for **2** causes only small changes (Table 4); the largest effect was found for **6**, where in neat acetonitrile τ_{em} is reduced to 1.1 ms. The lifetime of **2** in ethanol changes little (<20%) when the

Table 3 Selected bond lengths (Å) and angles (°) for [$tp_2Tb(\mu-N_3)]_4$ (**7**)

Tb(1)–N(22)	2.507(2)	Tb(1)–N(7)	2.520(2)
Tb(1)–N(27)	2.534(2)	Tb(1)–N(2)	2.545(2)
Tb(1)–N(32)	2.458(2)	Tb(1)–N(12)	2.500(2)
Tb(1)–N(80)	2.423(2)	Tb(1)–N(90)	2.425(2)
Tb(2)–N(47)	2.454(2)	Tb(2)–N(67)	2.480(2)
Tb(2)–N(52)	2.492(2)	Tb(2)–N(62)	2.531(2)
Tb(2)–N(72)	2.533(2)	Tb(2)–N(42)	2.557(2)
Tb(2)–N(92)	2.414(2)	Tb(2)–N(82)	2.450(2)
N(80)–N(81)	1.169(3)	N(81)–N(82)	1.178(3)
N(90)–N(91)#1	1.171(3)	N(91)–N(90)#1	1.171(3)
N(91)–N(92)	1.174(3)		
N(80)–Tb(1)–N(90)	78.66(7)	N(80)–Tb(1)–N(32)	140.69(7)
N(90)–Tb(1)–N(32)	74.66(7)	N(80)–Tb(1)–N(12)	73.83(7)
N(90)–Tb(1)–N(12)	137.69(7)	N(32)–Tb(1)–N(12)	143.34(7)
N(80)–Tb(1)–N(22)	74.85(7)	N(90)–Tb(1)–N(22)	78.91(7)
N(32)–Tb(1)–N(22)	72.10(7)	N(12)–Tb(1)–N(22)	122.43(6)
N(80)–Tb(1)–N(7)	86.61(7)	N(90)–Tb(1)–N(7)	73.90(7)
N(32)–Tb(1)–N(7)	112.46(7)	N(12)–Tb(1)–N(7)	72.98(6)
N(22)–Tb(1)–N(7)	149.61(7)	N(80)–Tb(1)–N(27)	111.38(7)
N(90)–Tb(1)–N(27)	146.02(7)	N(32)–Tb(1)–N(27)	78.59(6)
N(12)–Tb(1)–N(27)	75.16(6)	N(22)–Tb(1)–N(27)	73.16(6)
N(7)–Tb(1)–N(27)	136.91(6)	N(80)–Tb(1)–N(2)	146.20(7)
N(90)–Tb(1)–N(2)	118.62(7)	N(32)–Tb(1)–N(2)	72.96(7)
N(12)–Tb(1)–N(2)	74.73(6)	N(22)–Tb(1)–N(2)	134.15(7)
N(7)–Tb(1)–N(2)	72.57(7)	N(27)–Tb(1)–N(2)	71.59(6)
N(92)–Tb(2)–N(82)	75.43(7)	N(92)–Tb(2)–N(47)	73.32(7)
N(82)–Tb(2)–N(47)	136.93(7)	N(92)–Tb(2)–N(67)	138.75(7)
N(82)–Tb(2)–N(67)	73.96(7)	N(47)–Tb(2)–N(67)	146.18(7)
N(92)–Tb(2)–N(52)	88.88(7)	N(82)–Tb(2)–N(52)	75.91(7)
N(47)–Tb(2)–N(52)	74.60(7)	N(67)–Tb(2)–N(52)	109.47(7)
N(92)–Tb(2)–N(62)	113.06(7)	N(82)–Tb(2)–N(62)	144.09(7)
N(47)–Tb(2)–N(62)	76.58(7)	N(67)–Tb(2)–N(62)	79.01(7)
N(52)–Tb(2)–N(62)	136.47(6)	N(92)–Tb(2)–N(72)	75.11(7)
N(82)–Tb(2)–N(72)	79.67(7)	N(47)–Tb(2)–N(72)	118.96(7)
N(67)–Tb(2)–N(72)	72.76(6)	N(52)–Tb(2)–N(72)	153.52(6)
N(62)–Tb(2)–N(72)	69.94(6)	N(92)–Tb(2)–N(42)	147.72(7)
N(82)–Tb(2)–N(42)	121.97(7)	N(47)–Tb(2)–N(42)	76.64(6)
N(67)–Tb(2)–N(42)	73.26(6)	N(52)–Tb(2)–N(42)	71.84(6)
N(62)–Tb(2)–N(42)	70.24(6)	N(72)–Tb(2)–N(42)	131.37(6)
N(80)–N(81)–N(82)	178.6(2)	N(90)#1–N(91)–N(92)	177.7(3)

Table 4 Emission properties of the Tb complexes[a]

Compound	Solvent	I_{em}[b]	τ_{em}/ms
2	Cyclohexane	1	1.7
	Dichloromethane	0.9	1.7[c]
	Acetonitrile	0.8	1.6[c],[d]
	Ethanol	0.7	1.6
4	Dichloromethane	0.8	1.7[c]
5	Dichloromethane	0.1	1.7
6	Dichloromethane	0.01	≈1.3
7	Dichloromethane	0.5	1.6

[a] In air-saturated solution at room temperature. [b] Excitation at 250 nm. [c] Same value in the absence or presence of air. [d] Same value in the presence of water (0.1–1 M).

temperature is decreased from 25 to −196 °C, whereas the relative yield of emission increases 2–3 fold. The lifetimes of the Eu($^5D_0$) and Tb($^5D_4$) excited levels of novel polydentate hemispherands are essentially independent of temperature,[7] but quenched by C–H vibrational modes.[8]

Energy transfer and the effect of water. Eu and Tb complexes are known to exhibit narrow emission bands with a major peak at 620 and 550 nm, respectively.[4–12] The luminescence intensity of the *p*-bromobenzoate **5** is significantly smaller and even smaller for the *p*-nitrobenzoate **6** (Table 4). This indicates a deactivation process competing with energy transfer from the ligand-centered level to the Tb centered level; the rate constants are k_q and k_{et}, respectively (Scheme 1). We propose that this enhanced deactivation into the ground state (S_0) is caused by charge delocalization in the excited singlet state (S_1). This charge transfer is largest for complex **6**, where the ligand contains the strongly electron-accepting *p*-nitrobenzoate.

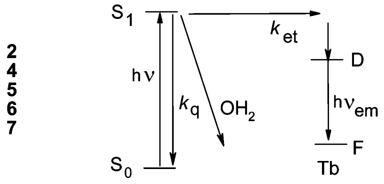

Scheme 1

Since water quenches the luminescence of Eu(III) or Tb(III) compexes,[4–6] we studied the effect of aqueous solution in two cases. The peak intensity of **2** in acetonitrile becomes smaller on addition of water (pH 7), but the plot of $1/I_{em}$ *vs.* the water concentration is upward curved. From the initial part of this plot a half-concentration for 50% quenching of $[H_2O]_{1/2} \approx 0.9$ M was estimated. The effect of quenching of **2** in ethanol is smaller, resulting in $[H_2O]_{1/2} \approx 3$ M. On the other hand, the lifetime remains essentially constant in the absence or presence of water. We therefore conclude that water reacts with the S_1 state (Scheme 1) or replaces a ligand. Generally, efficient radiationless deactivation takes place *via* O–H vibrational modes.[4–6]

Conclusions

The ligand hydrotris(pyrazolyl)borate can react with lanthanide(III) ions to give a seven-coordinate 1:1 complex or a eight-coordinate 1:2 complex, depending upon the presence of other ligands in the reaction mixture. In complexes **1** and **3**, each gadolinium is coordinated by four oxygen atoms from carboxylate groups and three nitrogen atoms from a hydrotris(pyrazolyl)borate ligand, and is seven coordinate. The same is also true in Tb complexes **2**, **4**, **5** and **6**. In terbium–azide complex **7**, each terbium is coordinated by six nitrogen atoms from two hydrotris(pyrazolyl)borate ligands and two nitrogen atoms from azido group which are acting as bridging, making each terbium eight coordinate. Complexes **1** and **2** are essentially isostructural and isomorphous, crystallizing in the triclinic space group $P\bar{1}$. Similarly, complexes **3**, and **4** are isostructural and isomorphous, also crystallizing in the triclinic space group $P\bar{1}$. The luminescence lifetime studies on terbium complexes show that the lifetime of the first-order emission decay is τ_{em} = 1.6–1.7 ms. Variation of the bridging ligands in dichloromethane or variation of the solvent for **2** causes only small changes.

Acknowledgements

This work was supported by UGC, New Delhi, India. U. P. S. is also grateful to the Alexander von Humboldt Foundation, Germany for financial support as a AvH visiting scientist and Prof. Karl Wieghardt for providing laboratory space as well as helpful discussion and encouragement during stay in his laboratory.

References

1 (*a*) S. Aime, M. Botta, M. Fasano and E. Terreno, *Chem. Soc., Rev.*, 1998, **27**, 19; (*b*) N. Sabbatini, M. Guardigli and J.-M. Lehn, *Coord. Chem. Rev.*, 1993, **123**, 201; (*c*) A. K. Saha, K. Kross, E. D. Kloszewski, D. A. Upson, J. L. Toner, R. A. Snow, C. D. V. Black and V. C. Desai, *J. Am. Chem. Soc.*, 1993, **115**, 11032; (*d*) A. P. de Silva, H. Q. N. Gunaratne and T. E. Rice, *Angew. Chem., Int. Ed. Engl.*, 1996, **35**, 2116; (*e*) M. A. Mortellaro and D. G. Nocera, *J. Am. Chem. Soc.*, 1996, **188**, 7414.

2 (*a*) R. B. Lauffer, *Chem. Rev.*, 1987, **87**, 901; (*b*) M. Inoue, R. E. Navarro, M. Inoue and Q. Fernando, *Inorg. Chem.*, 1995, **34**, 6074; (*c*) D. E. Reichert, R. D. Hancock and M. J. Welch, *Inorg. Chem.*, 1996, **35**, 7013; (*d*) D. H. Powell, O. M. Ni Dhubhghaill, D. Pubanz, L. Helm, Y. S. Lebedev, W. Schlaepfer and A. E. Merbach, *J. Am. Chem. Soc.*, 1996, **118**, 9333.

3 V. Balzani, A. Juris, M. Venturi, S. Campagna and S. Serroni, *Chem. Rev.*, 1996, **96**, 759.

4 V. Balzani, E. Berghmans, J.-M. Lehn, N. Sabbatini, R. Terörde and R. Ziessel, *Helv. Chim. Acta*, 1990, **73**, 2083.

5 (*a*) N. Sabbatini, S. Dellonte, M. Ciano, A. Bonazzi and V. Balzani, *Chem. Phys. Lett.*, 1984, **107**, 212; (*b*) B. Alpha, J.-M. Lehn and G. Mathis, *Angew. Chem. Int. Ed. Engl.*, 1987, **99**, 266; (*c*) B. Alpha, V. Balzani, J.-M. Lehn, S. Perathoner and N. Sabbatini, *Angew. Chem., Int. Ed. Engl.*, 1987, **99**, 1266; (*d*) J.-M. Lehn, M. Pietraszkiewicz and J. Karpiuk, *Helv. Chim. Acta*, 1990, **73**, 106.

6 M. J. Remuiñán, H. Román, M. T. Alonso and J. C. Rodrígues-Ubis, *J. Chem. Soc., Chem. Commun.*, 1993, 1099.

7 C. Piguet, J.-C. G. Bünzli, G. Bernardinelli, G. Hopfgartner, S. Petoud and O. Schaad, *J. Am. Chem. Soc.*, 1996, **118**, 6681.

8 M. P. O. Wolbers, F. C. J. M. van Veggel, B. H. M. Snellink-Rüel, J. W. Hofstraat, F. A. J. Geurts and D. N. Reinhoudt, *J. Am. Chem. Soc.*, 1997, **119**, 138.

9 S. I. Klink, L. Grave, D. N. Reinhoudt, F. C. J. M. van Veggel, M. H. V. Werts, F. A. J. Geurts and J. Hofstraat, *J. Phys. Chem.*, 2000, **104**, 5457.

10 R. G. Lawrence, C. J. Jones and R. A. Kresinski, *J. Chem. Soc., Dalton Trans.*, 1996, 501.

11 D. A. Bardwell, J. C. Jeffery, P. L. Jones, J. A. McCleverty, E. Psillakis, Z. Reeves and M. D. Ward, *J. Chem. Soc., Dalton Trans.*, 1997, 2079.

12 P. L. Jones, A. J. Amoroso, J. C. Jeffery, J. A. McCleverty, E. Psillakis, L. H. Rees and M. D. Ward, *Inorg. Chem.*, 1997, **36**, 10.

13 (*a*) P. R. Selvin, J. Jancarik, M. Li and L.-W. Hung, *Inorg. Chem.*, 1996, **35**, 700; (*b*) A. Dossing, H. Toftlund, A. Hazell, J. Bourassa and P. C. Ford, *J. Chem. Soc., Dalton Trans.*, 1997, 335.

14 (*a*) D. L. Reger, J. A. Lindeman and L. Lebioda, *Inorg. Chem.*, 1988, **27**, 3923; (*b*) D. L. Reger, J. A. Lindeman and L. Lebioda, *Inorg. Chim. Acta*, 1987, **139**, 73; (*c*) L. Jin, S. Lu and S. Lu, *Polyhedron*, 1996, **15**, 4069; (*d*) M. N. Tahir, D. Ülkü, C. Ünaleroglü and E. M. Mövsümov, *Acta Crystallogr., Sect. C*, 1996, **52**, 1449; (*e*) L. Jin, R. Wang, L. Li, S. Lu and S. Huang, *Polyhedron*, 1999, **18**, 487; (*f*) G. Arici, D. Ülkü, M. N. Tahir and C. Ünaleroglü, *Acta Crystallogr., Sect. C*, 1999, **55**, 198; (*g*) Y. Cui, F. Zheng, Y. Qian and J. Huang, *Inorg. Chim. Acta*, 2001, **312**, 220; (*h*) D. L. Reger, S. J. Knox, J. A. Lindeman and L. Lebioda, *Inorg. Chem.*, 1990, **29**, 416.

15 (*a*) R. Vicente, A. Escuer, J. Ribas, M. S. El Fallah, X. Solans and M. Font-Bardia, *Inorg. Chem.*, 1993, **32**, 1920; (*b*) J. Ribas, M. Monfort, C. Diaz, C. Bastos and X. Solans, *Inorg. Chem.*, 1994, **33**, 484&–3557; (*c*) J. Ribas, M. Monfort, R. Costa and X. Solans, *Inorg. Chem.*, 1993, **32**, 695; (*d*) R. Cortes, M. K. Urtiaga, L. Lezama, J. L. Pizarro, A. Goni, M. I. Arriortua and T. Rojo, *Inorg. Chem.*, 1994, **33**, 4009; (*e*) A. Escuer, R. Vicente, M. S. El Fallah, J. Ribas, X. Solans and M. Font-Bardia, *J. Chem. Soc., Dalton Trans.*, 1993, 2975.

16 H.-Z. Kou, D.-Z. Liao, P. Cheng, Z.-H. Jiang, S.-P. Yan and G.-L. Wang, *Synth. React. Inorg. Met.-Org. Chem.*, 1998, **28**, 405.

17 D. D. Perrin, W. L. Armarego and D. R. Perrin, *Purification of Laboratory Chemicals*, Pergamon, New York, 2nd edn., 1980.

18 S. Trofimenko, *J. Am. Chem. Soc.*, 1967, **89**, 6288.

19 (*a*) H. Görner and A. K. Chibisov, *J. Chem. Soc., Faraday. Trans.*, 1998, **94**, 2557; (*b*) A. K. Chibisov and H. Görner, *Chem. Phys.*, 1998, **237**, 425.

20 ShelXTL 5, Siemens Analytical X-Ray Instruments, Inc. 1994.

21 K. Nakamoto, *Infrared Spectra of Inorganic and Coordination Compounds*, Wiley, New York, 3rd edn., 1986.

22 (*a*) P. Starynowicz, *Acta Crystallogr., Sect. C*, 1992, **48**, 4; (*b*) H. Schumann, C. Janiak and J. Pickardt, *J. Organomet. Chem.*, 1988, **349**, 117; (*c*) F. A. Maunter and H. Krischner, *Monatsh. Chem.*, 1990, **12**, 781; (*d*) P. Starynowicz, K. Bukietynska, W. Ryba-Romanowski, G. Dominiak-Dzik and S. Golab, *Polyhedron*, 1994, **13**, 1069; (*e*) P. Starynowicz, *Acta Crystallogr., Sect. C*, 1991, **47**, 4.

23 Abbreviations used are as follows: (tp), hydrotris(1-pyrazolyl)borate (1−); OBz, benzoate; *p*, *para*.